Supplemental Figures S1-S19 with legends.

Figure S1. ER+ breast cancer cells lie dormant during estrogen depletion *in vivo* and retain tumor-initiating capacity. MCF-7 cells were s.c. injected into ovx mice, and mice were immediately randomized to s.c. implantation of an E2 pellet (black) or sham control (blue/red). After 10 wk, control mice remaining were then randomized to E2 pellet (blue) or control (red). Tumor volumes were measured twice weekly.

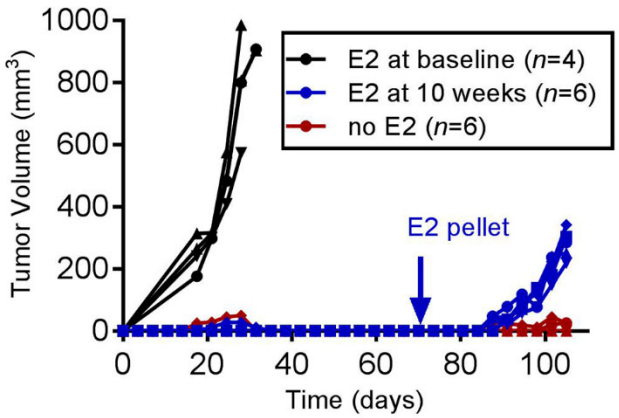

Figure S2. Individual tumor regression and growth curves for mice with estrogen-withdrawn and estrogen-retreated xenografts. (A-E) Ovx mice bearing bilateral E2-driven orthotopic tumors measuring ~400 mm^3 were treated with estrogen withdrawal starting on Day 0. Tumor volumes were measured twice weekly. Each line represents one tumor. Summarized data are shown in Fig. 1B. **(F-H)** Ovx mice bearing E2-driven orthotopic tumors were treated with estrogen withdrawal as above. After 90 d of estrogen withdrawal, mice were retreated with E2 via s.c. pellet on Day 0. Tumor volumes were measured twice weekly. Each line represents one tumor.

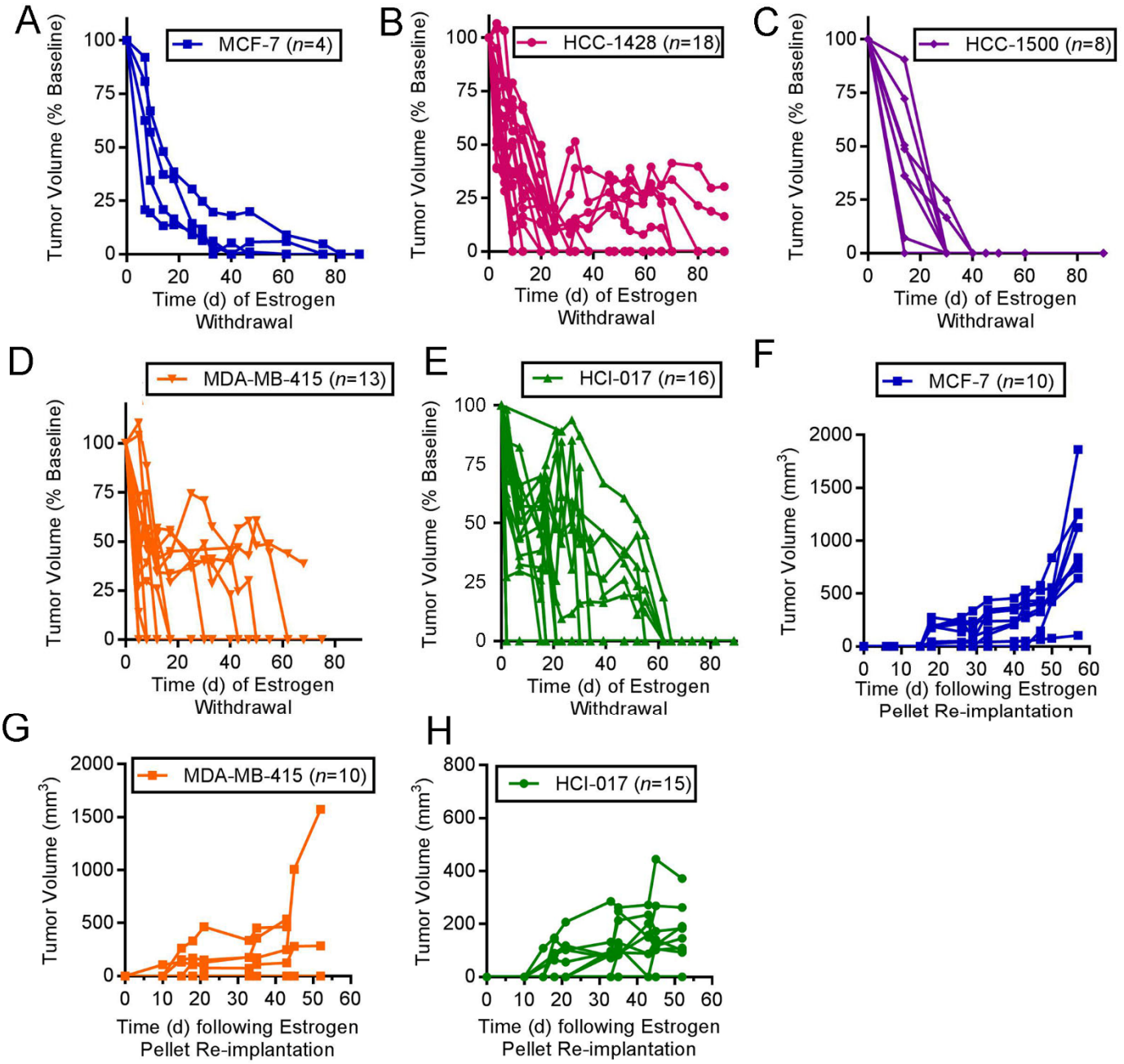

Figure S3. Immunohistochemical analysis of Ki67, cleaved caspase 3/7, and ER in ER+ breast cancer xenografts. Representative images for Ki67 **(A)**, cleaved caspase 3/7 **(B)**, and ER **(C)** IHC staining of FFPE xenografts are shown. Tumor specimens were harvested from ovx mice following 0, 6, or 90 d of estrogen withdrawal. Summarized data for (A) and (B) are shown in Fig. 1F-H. Summarized data for (C) are shown in (D). Data are shown as mean of triplicates + SD. *p≤0.05 by t-test. n.s.- not significant.

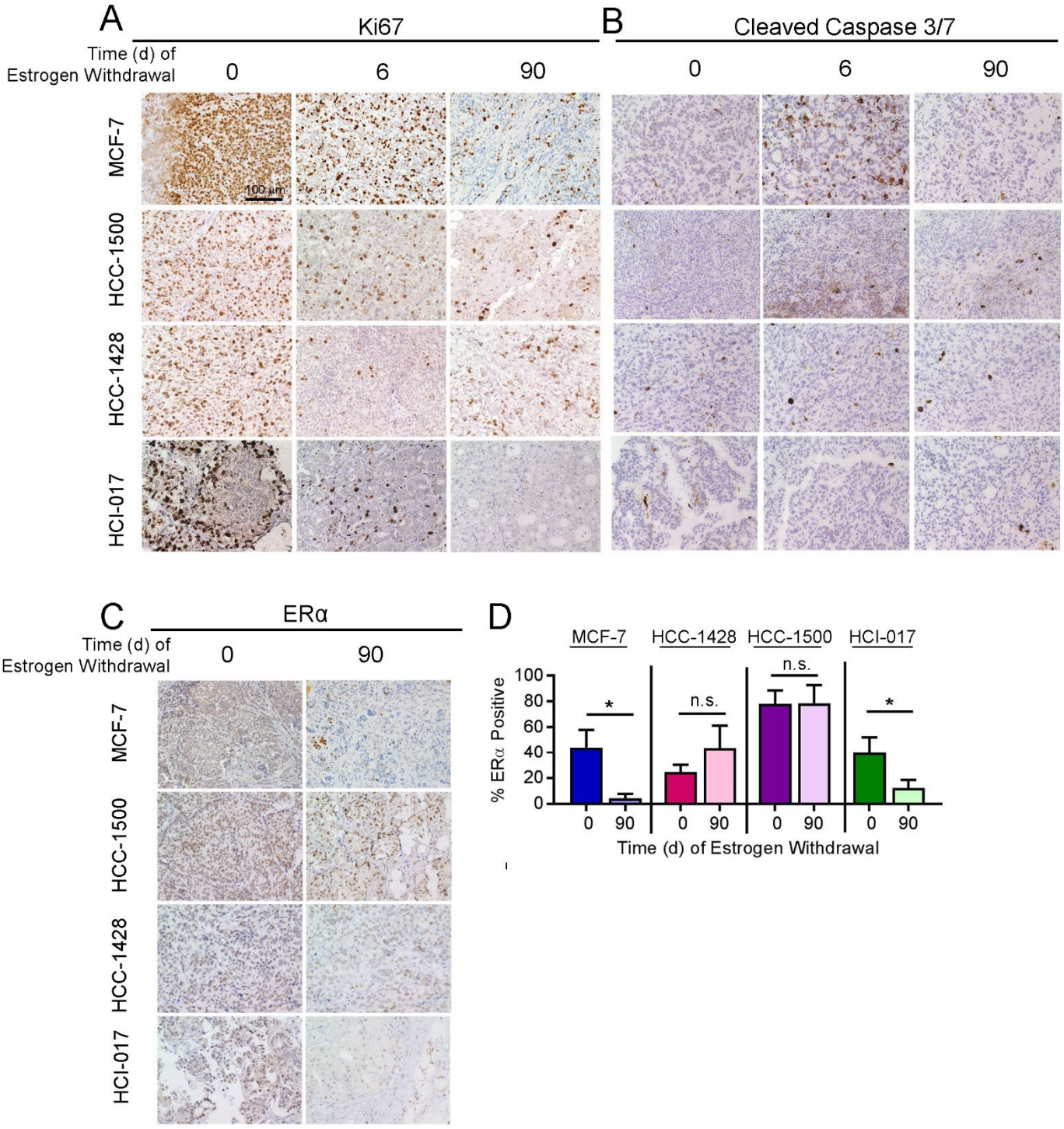

Figure S4. Gene Set Variation Analysis (GSVA) of RNA sequencing data from ER+ breast cancer xenografts. RNA extracted from MCF-7 or HCC-1428 tumors after 0 or 90 d of estrogen withdrawal (*n*=3-4 tumors/time point) was analyzed by sequencing. Gene set variation analysis (GSVA) of whole-transcriptome expression profiles of clinically dormant tumors (Day 90) compared to baseline (Day 0) was performed using unsupervised sample-wise enrichment analysis of common metabolic and signaling gene sets [selected from the Hallmarks (HM), Gene Ontology (GO), Reactome (RM), or Motif Gene Sets (C3) collections]. Vertical dotted line indicates adjusted p=0.2 threshold, which is below the recommended cutoff of p=0.25 for significance in Gene Set Enrichment Analysis (1). Summarized data are shown in Fig. 2A.

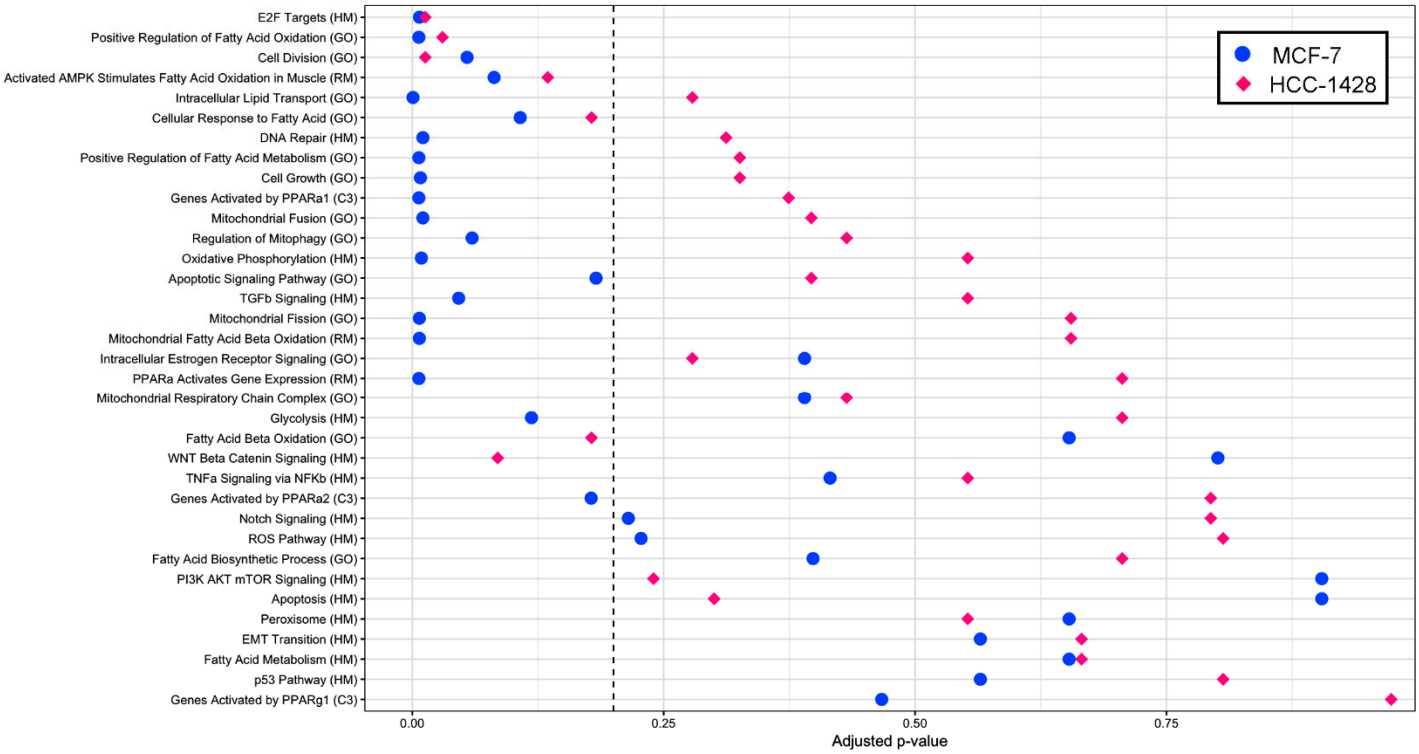

Figure S5. RNA sequencing analysis of ER+ BC xenografts. RNA was extracted from macrodissected sections of FFPE MCF-7 **(A)** or HCC-1428 **(B)** tumors harvested from ovx mice after 0, 6, or 90 d of estrogen withdrawal (EW; *n*=3-4 tumors/time point), and analyzed by sequencing. Genes that were significantly differentially expressed (q≤0.05, $|\log_2 FC|>1.0$) between Day 6 (acute EW) and Day 0 (baseline) (blue and yellow circles), or between Day 90 (dormant) vs. Day 0 (baseline) (red and green circles) were identified; numbers of these genes are indicated in Venn diagrams. *AMPKα2 (PRKAA2) mRNA was upregulated at Day 90, but not Day 6, compared to baseline in both tumor models. GSVA results are shown in Figure 2A and Figure S4.

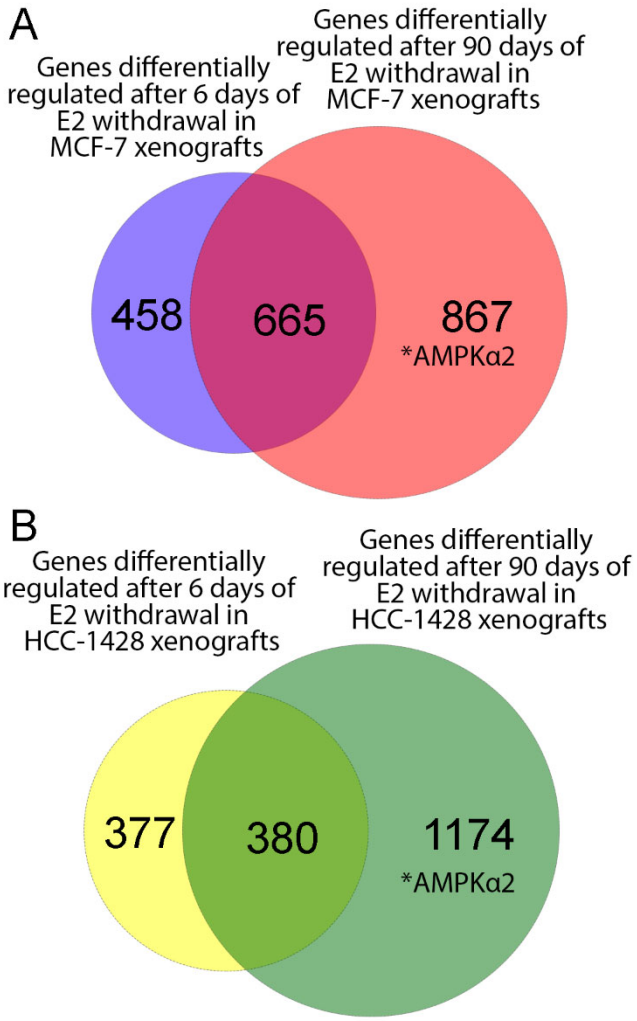

Figure S6. Immunohistochemical analysis of AMPKα2 and P-ACC in ER+ breast cancer xenografts. Representative images for AMPKα2 **(A)** and P-ACC$_{Ser79}$ **(B)** IHC staining of FFPE xenografts are shown. Tumor specimens were harvested from ovx mice following 0, 6, or 90 d of estrogen withdrawal. Summarized data are shown in Fig. 2C/D.

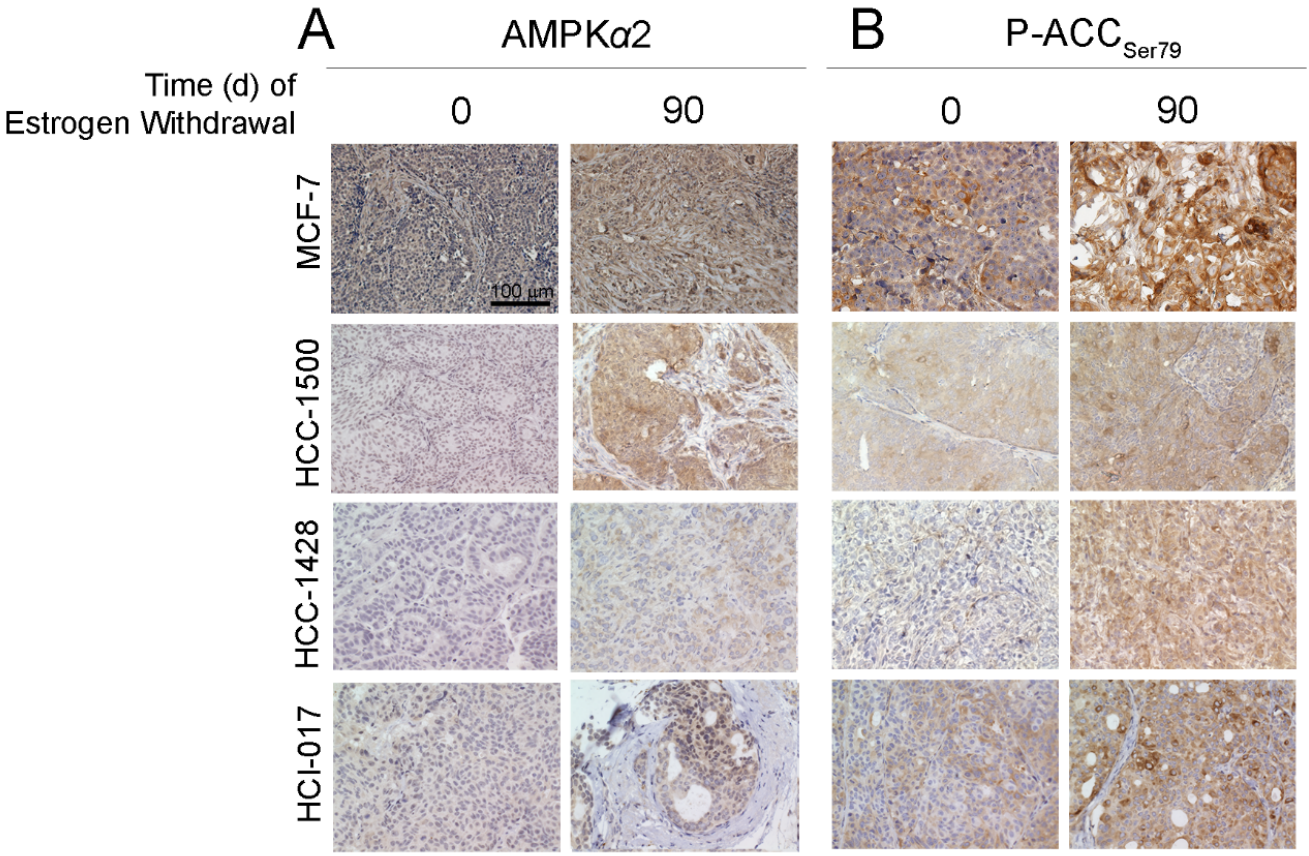

Figure S7. Effects of dormancy on mTORC1 activation in ER+ breast tumors. (A) MCF-7 tumors were harvested from ovx mice after 0 or 90 d of estrogen withdrawal (EW). FFPE tumors specimens were analyzed by IHC for phospho-S6. Representative images are shown. Proportions of positively-stained cells were measured using HaloVelocity software in 3 images per tumor; values were averaged within each tumor (3 tumors per group). Quantification is shown on right. Bars indicate mean ± SD. Groups were compared using *t*-test. **(B)** In a separate experiment, GFP+ MCF-7 tumors were harvested from ovx mice after 0, 3, 6, 12, or 90 d of EW (3 tumors per time point). Tumors were enzymatically digested into single-cell suspensions, stained using phospho-S6 antibody, and analyzed by flow cytometry. Proportions of GFP+ cells that were P-S6-positive were measured. Data are shown as mean of triplicates ± SD. **p*≤0.05 by Bonferroni multiple comparison-adjusted posthoc test.

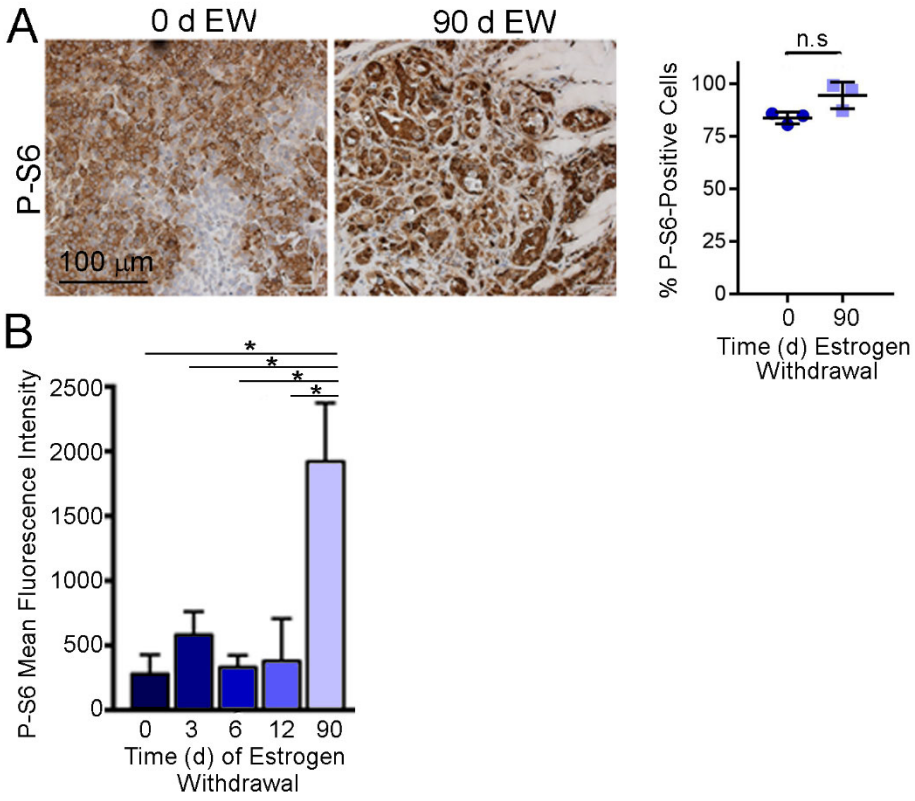

Figure S8. Residual ER+ breast tumor cells exhibit a transcriptional signature of FAO following presurgical anti-estrogen treatment. Human ER+ breast tumor etomoxir *t*-statistics were calculated using the 915 genes non-cell cycle-related gene signature of etomoxir response from MCF-7 cells. There were 863 (GSE20181), 629 (GSE71791), and 632 (GSE111563) non-cell cycle-related genes available on each platform. Groups were statistically analyzed by repeated measures ANOVA followed by Tukey's multiple comparison-adjusted posthoc test between time points (A) or paired *t*-test (B/C). Red bars indicate mean values.

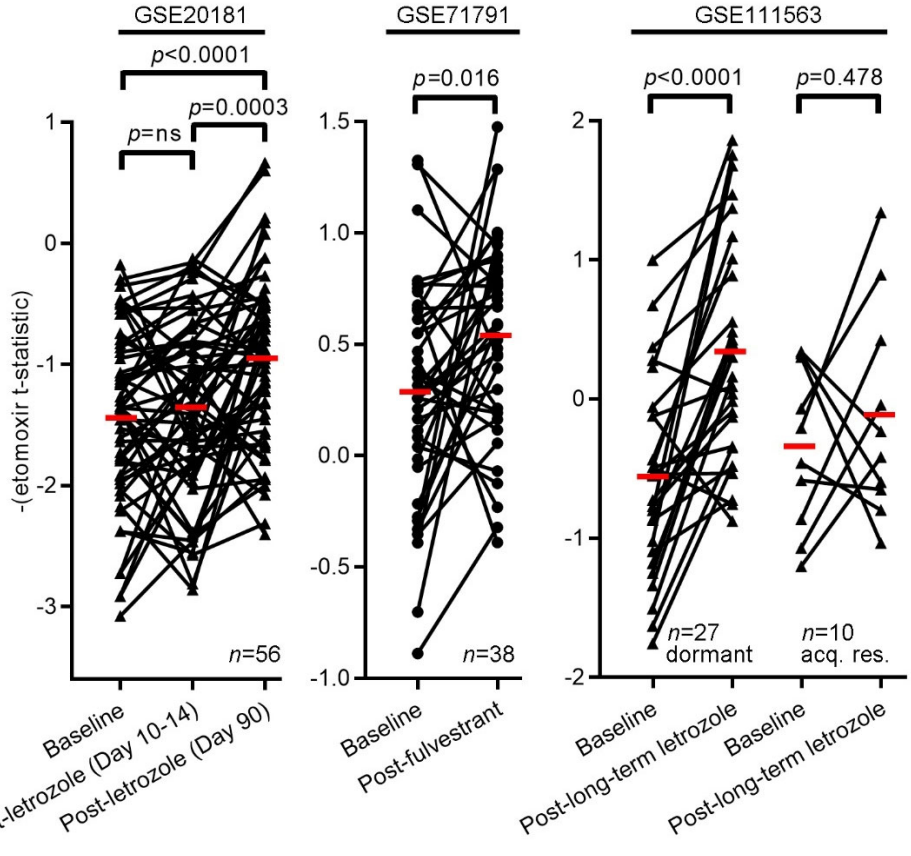

Figure S9. Clinically dormant tumor cells exhibit markers of increased mitochondrial content and activity. (A) Normalized mRNA read counts for mitochondria-encoded genes extracted from RNA-seq data. **(B-C)** Mitochondria in tumor specimens harvested after 0 or 90 d of EW were stained with TOM20-AF594 by immunofluorescence. Mitochondrial count (B) and length (C) per cell (from ≥30 cells) were calculated in each of 3 tumors per group. *$p \leq 0.05$ by *t*-test. (D) Representative IHC images for CPT1α staining of tumors. Summarized data are shown in Fig. 2H.

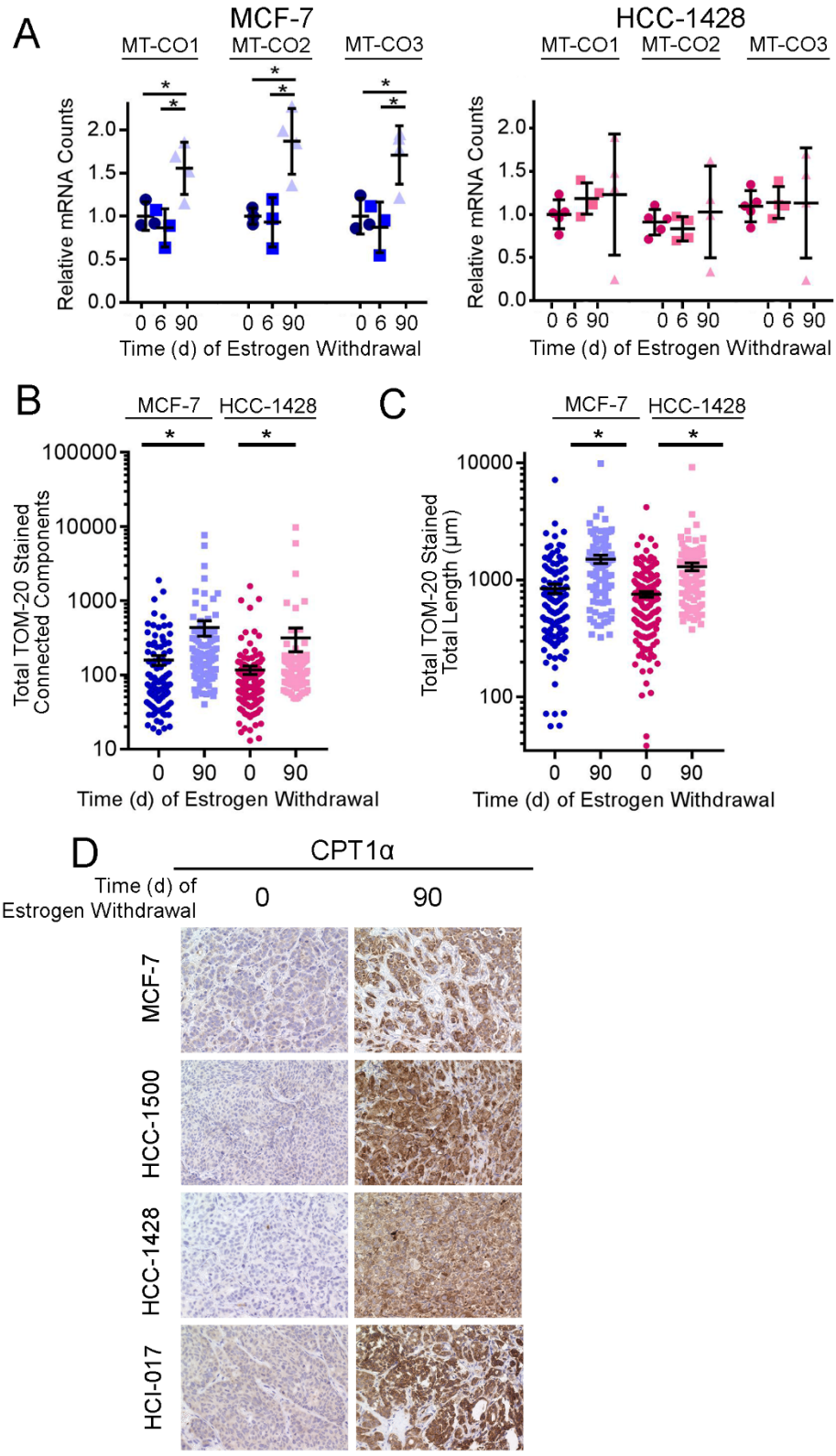

Figure S10. AMPK is required for hormone deprivation-induced increases in cellular respiration in ER+ breast cancer cells. (A-B) Cells were transiently transfected with siRNA targeting AMPKα1 and/or AMPKα2, or non-silencing control. Three days later, lysates were harvested and analyzed by immunoblot. **(C-E)** MCF-7 cells were pre-treated with hormone-depleted (HD) medium ± 1 nM E2 for 12 d, then transfected with siRNA against AMPKα1 and AMPKα2, or non-silencing control. Cells were maintained in growth medium or HD medium for an additional 3 d, then assayed for cellular respiration. Basal OCR (B), spare capacity (C), and ATP production (D) measurements were calculated. **(F)** Cells were seeded and treated as indicated. After 2-4 wk, relative cell number was determined by crystal violet assay. Data were normalized relative to each control-treated cell line. In (C-F), mean of triplicates + SD is shown. *$p \leq 0.05$ by Bonferroni multiple comparison-adjusted posthoc test (C-E) or *t*-test (F). n.s.- not significant.

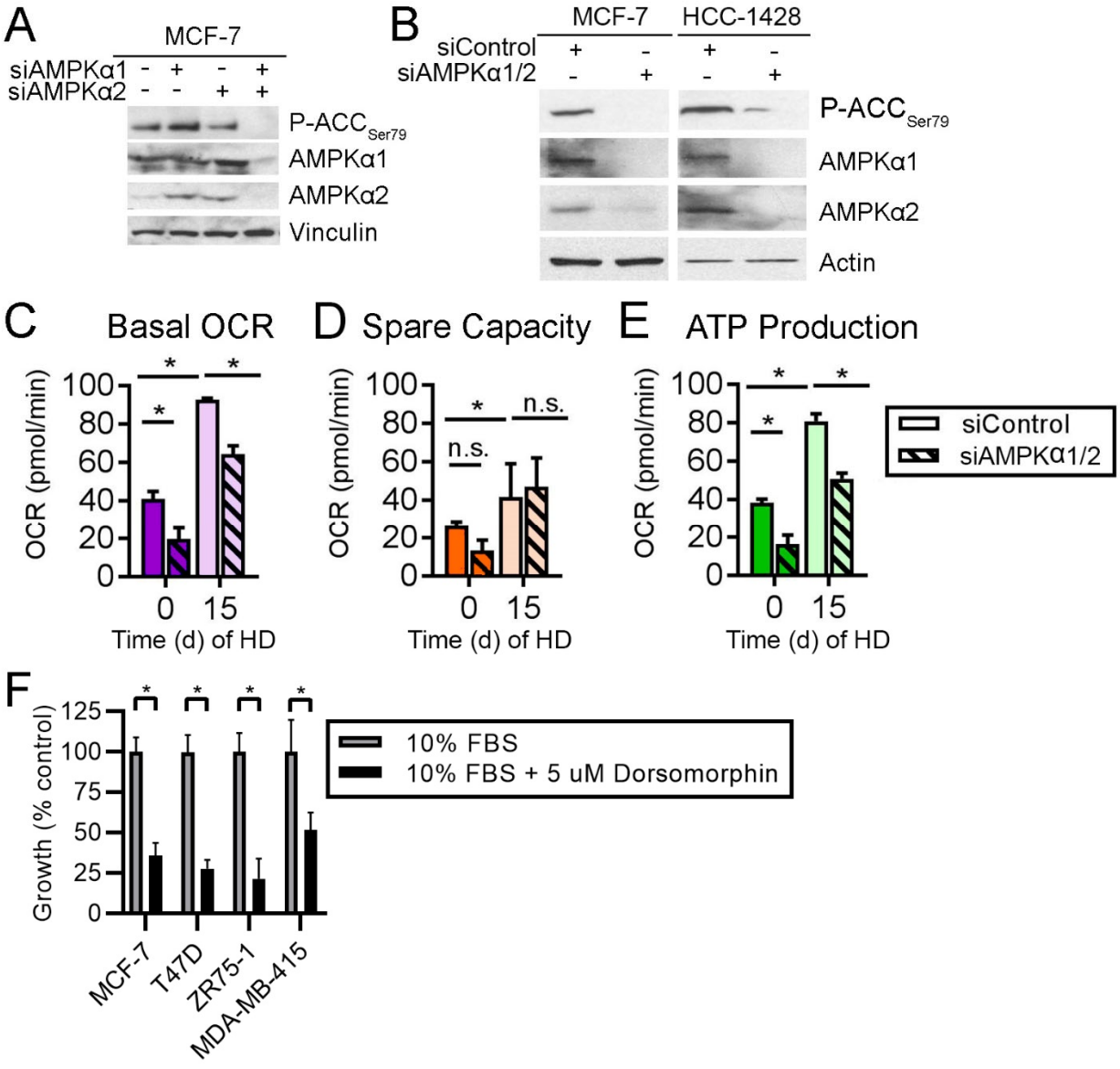

Figure S11. Inhibition of fatty acid oxidation hastens regression of ER+ breast tumors following estrogen withdrawal. Ovx mice bearing orthotopic bilateral E2-driven breast tumors (~400 mm^3) were randomized to treatment with estrogen withdrawal (EW) plus 14 d of drug treatment with ranolazine (50 mg/kg QD i.p.), etomoxir (50 mg/kg QD i.p.), perhexiline (15 md/kg BID i.p.), or vehicle control ("Early Treatment" as shown in Fig. 4C). Tumor volumes were measured twice weekly. Gray shading indicates the 14-day drug treatment period. EW continued after drug treatment ceased. Tumor volumes are shown as mean + SD. One drug treatment vs. vehicle is shown in each plot for visualization; vehicle group is the same in all plots within each model [(A) shows MCF-7; (B) shows HCC-1428]. Groups were compared using non-linear effect modeling depending on regression patterns. $p\text{-value}_{RD}$ reflects differences between rates of tumor regression; $p\text{-value}_{LT}$ reflects differences in tumor volume in the long term. For the MCF-7 model, tumors quickly regressed below the threshold for measurement, so long-term treatment effects could not be statistically evaluated.

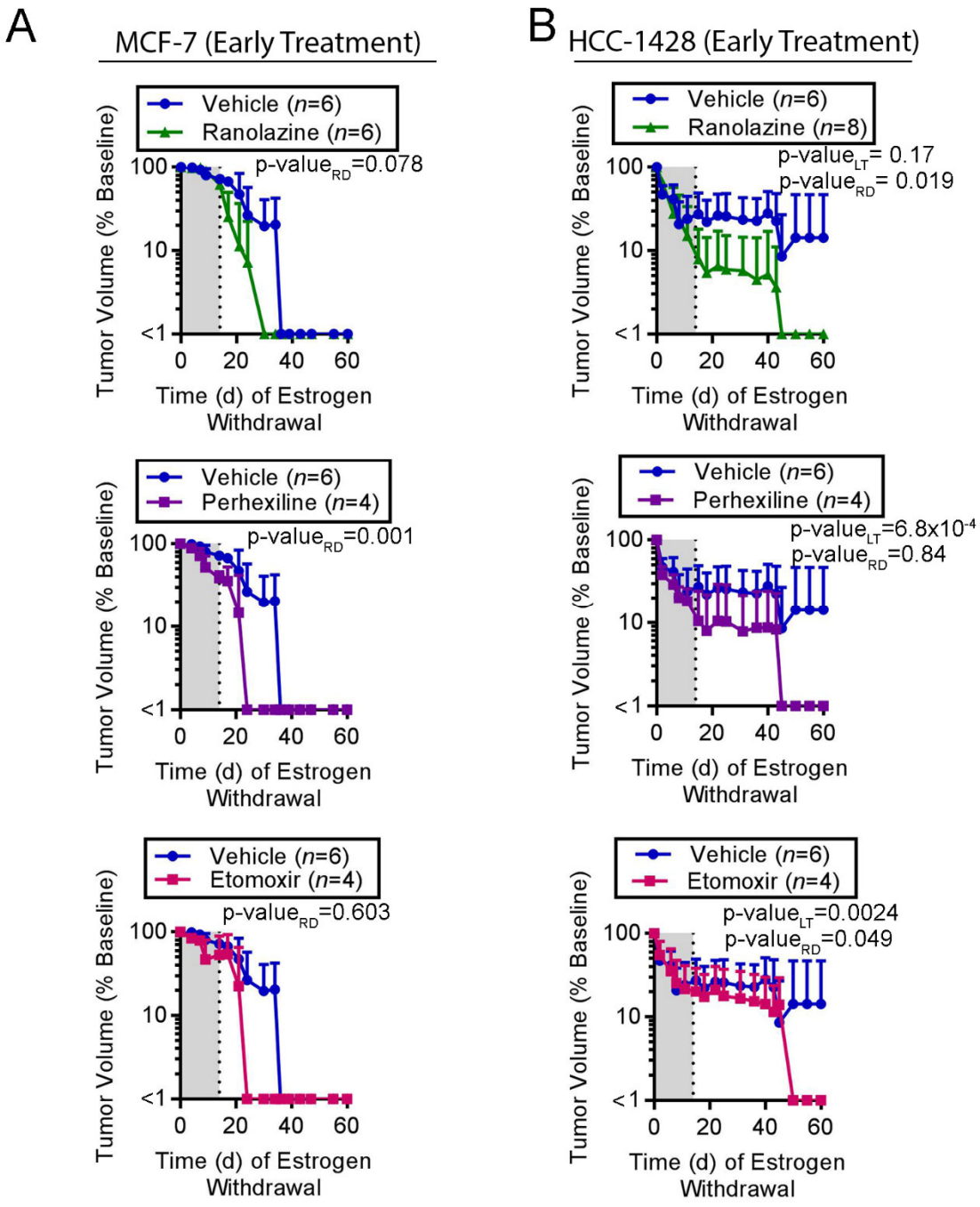

Figure S12. Pharmacologic analysis of metformin in ER+ breast cancer cells and tumors in mice. (A) Mice (*n*=5) were treated with metformin (~5 mg/d via drinking water) for 6 wk. Mice were euthanized. Blood was harvested and used to extract plasma. Tumor, muscle, and liver tissues were harvested. Plasma and tissues specimens were analyzed by LC-MS/MS to measure metformin concentrations. Bars indicate mean ± SD. **(B)** Ovx mice bearing E2-driven MCF-7 tumors were treated with EW for ~90 d, which caused complete regression of most tumors. In mice without palpable (residual) tumors, E2 supplementation was re-applied, and mice were simultaneously randomized to treatment ± metformin (~5 mg/d) on Day 0. Tumor volumes were measured twice weekly. Groups were compared using non-linear effect modeling depending on regression patterns. p-value$_{RD}$ reflects differences between rates of tumor growth. **(C)** Lysates from tumors harvested at the study endpoint in (B) were analyzed by immunoblot. **(D)** Cultured MCF-7 cells were treated with a dose range of metformin in growth medium for 24 h. Lysates were collected and analyzed by immunoblot. P-ACC and P-ULK1 were used as readouts of AMPK activity. **(E)** Cells were treated as in (D), then collected for measurement of concentrations of metformin (reported as mean ± SD of biological triplicates). **(F)** Cells were treated with hormone-depleted medium (HD) + 1 nM E2 ± 1 mM metformin for 21-28 d. Cells were then stained with crystal violet, and staining intensity was quantified. Data are shown as mean of triplicates + SD. *p≤0.05 by *t*-test compared to each control.

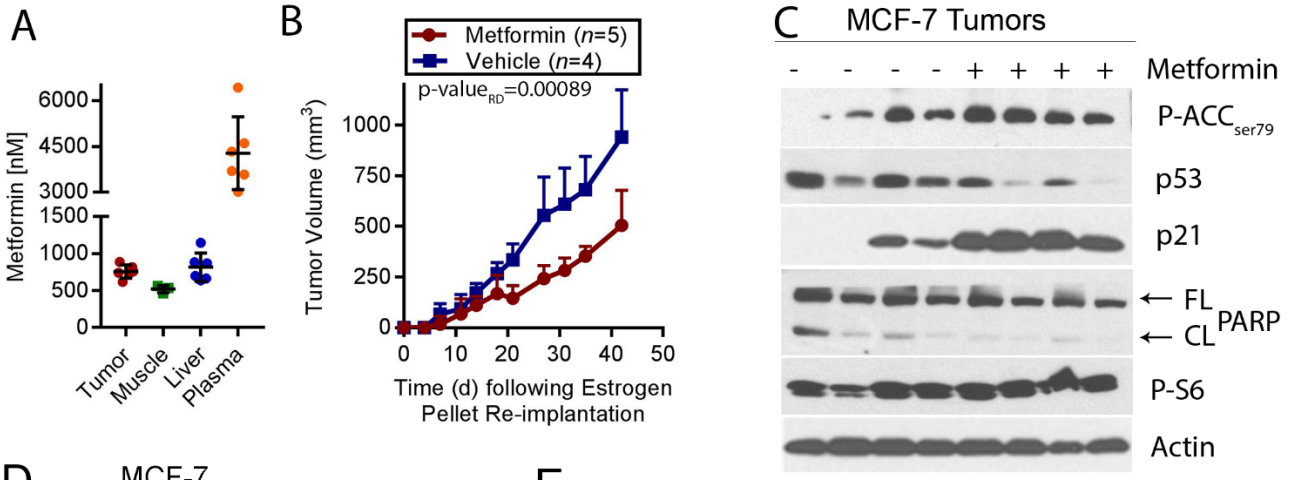

Concentration in Culture Media [μM]	Concentration in Cells [μM](+/- SD)
1	1.5 +/- 0.5
10	10.0 +/- 2.7
100	6.1 +/- 1.2
1,000	49.1 +/- 10.8
10,000	268.7 +/- 23.1

Figure S13. Metformin prevents estrogen withdrawal-induced regression of MDA-MB-415 ER+ breast tumors. (A) Ovx mice were orthotopically injected bilaterally with MDA-MB-415/luciferase cells, and implanted s.c. with an E2 pellet. Relative tumor cell numbers were serially measured by bioluminescence imaging. Tumors became palpable, and E2 pellets were removed on Day 117. Most tumors then regressed to a non-palpable state (indicated by gray shading). Each line represents an individual tumor. A representative bioluminescence image is shown at right after 90 d of EW. **(B)** Ovx mice bearing E2-driven MDA-MB-415/luciferase tumors (~400 mm^3) were treated with EW, and simultaneously randomized to treatment ± metformin (~5 mg/d via drinking water). Proportions of tumors that completely regressed (*i.e.*, non-palpable) over time are indicated. Kaplan-Meier curves were compared by log-rank test.

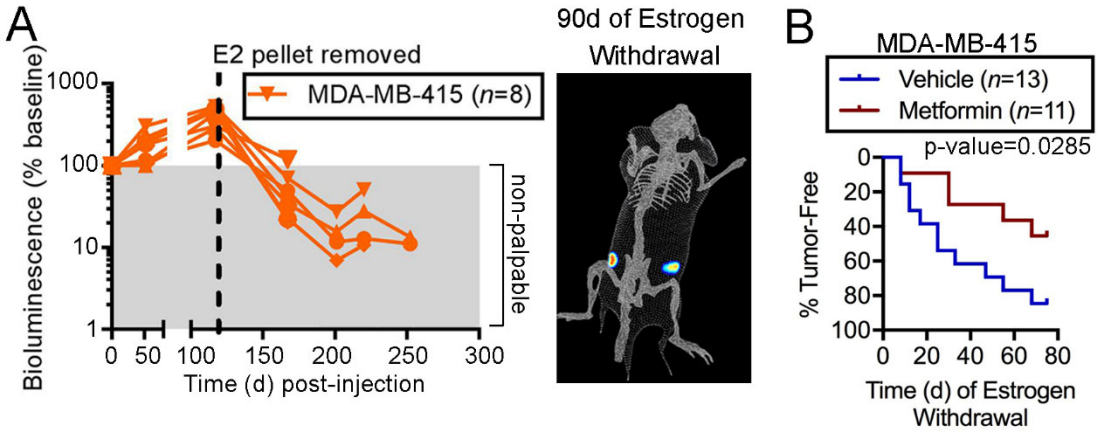

Figure S14. Metformin prevents estrogen withdrawal-induced regression of ER+ breast tumors. Ovx mice bearing orthotopic bilateral E2-driven tumors (~400 mm^3) were treated with EW, and simultaneously randomized to treatment ± metformin (~5 mg/d via drinking water). Tumor volumes are shown as mean ± SD. Groups were compared using non-linear effect modeling: $p\text{-value}_{RD}$ reflects differences between rates of tumor growth/regression; $p\text{-value}_{LT}$ reflects differences in tumor volume (*i.e.*, long-term treatment effect, or the proportion of tumor volume following treatment with respect to baseline tumor volume). Since metformin treatment was continued for the duration of the experiment, we focused on long-term treatment effects. However, MCF-7 and HCI-017 vehicle-treated tumors quickly regressed to below the limit of detection; thus, we could not measure long-term treatment effects (to generate $p\text{-value}_{LT}$), and instead measured short-term treatment effects to assess differences in rates of regression (to generate $p\text{-value}_{RD}$).

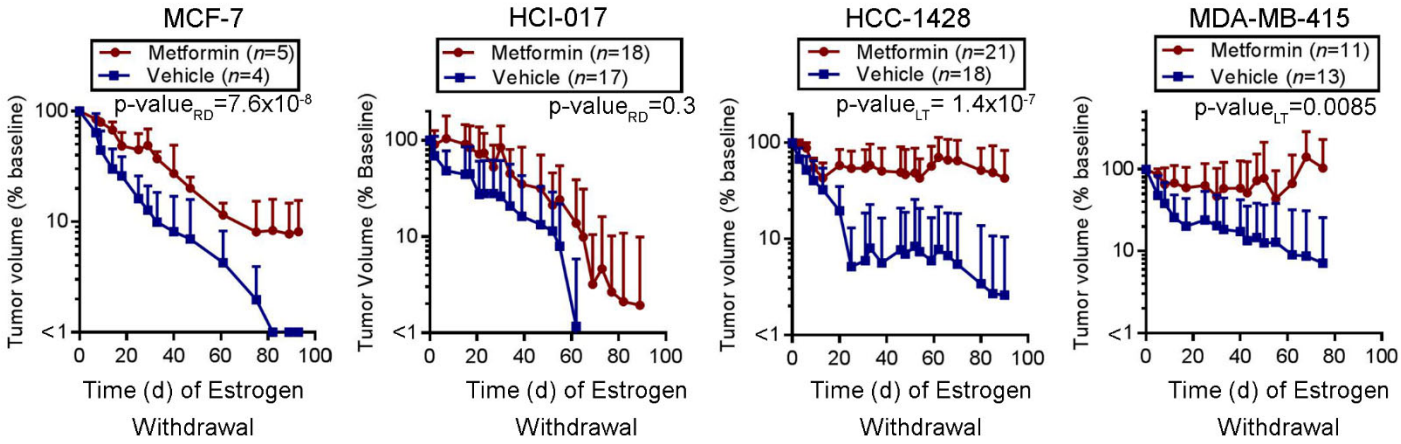

Figure S15. Metformin treatment does not significantly alter fasting levels of blood glucose, serum insulin, or serum free fatty acids in mice. Mice were treated ± metformin (~5 mg/d via drinking water) for 6 wk. Mice were fasted for 12 h overnight, then bled retroorbitally. Blood was used to measure concentrations of glucose **(A)**, or processed to extract serum. Serum was used to measure concentrations of insulin **(B)** and free fatty acids **(C)**. Each point represents one mouse. Bars indicate mean ± SD. Groups were compared by *t*-test. n.s.- not significant.

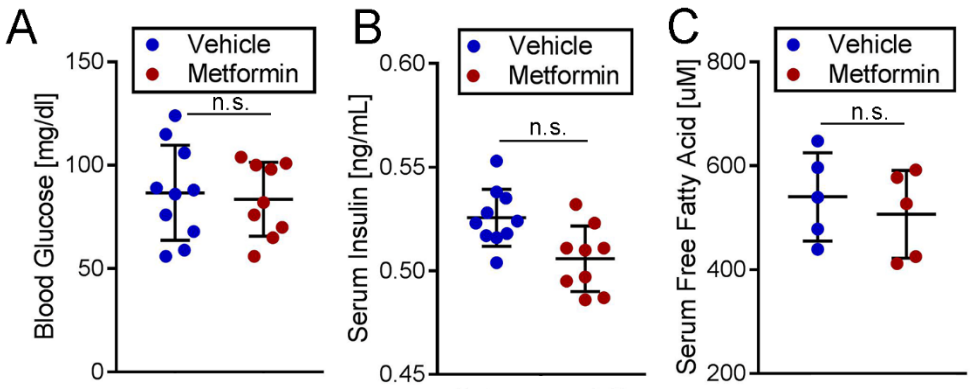

Figure S16. Immunohistochemical analysis of P-ACC in ER+ breast tumors from mice treated ± metformin. Representative images for P-ACC$_{Ser79}$ IHC staining of FFPE xenografts are shown. Tumor specimens were harvested from ovx mice following 12 d (MCF-7) or 6 d (HCC-1500, HCC-1428, HCI-017) of EW. For the duration of those 6-12 d, mice were randomized to receive metformin or vehicle control. Summarized data are shown in Fig. 5E.

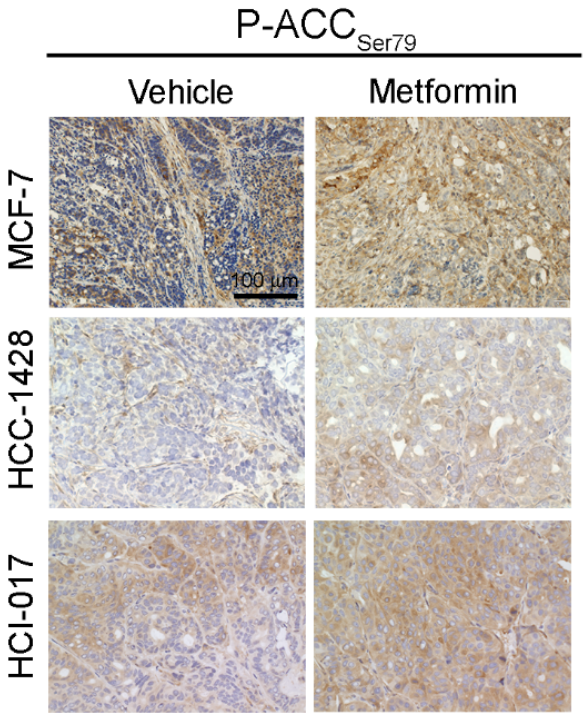

Figure S17. AMPK modulation does not alter growth/survival of HCC-1500 ER+ breast cancer cells or tumors. (A) HCC-1500 cells were treated with hormone-depleted medium (HD) ± 1 mM metformin for 21-28 d in triplicate. Relative cell numbers were quantified by Incucyte. Data are shown as mean + SD. **(B)** Ovx mice bearing orthotopic bilateral E2-driven HCC-1500/luciferase tumors (~400 mm^3) were treated with EW, and simultaneously randomized to treatment ± metformin (~5 mg/d via drinking water). Proportions of mice with complete tumor regression (*i.e.*, non-palpable) are indicated. Kaplan-Meier curves were compared by log-rank test. **(C)** Lysates from ER+ breast cancer cell lines were analyzed by immunoblot. P-ACC_{Ser79} and P-$ULK1_{Ser555}$ were used as readouts of AMPK activity. **(D)** Cells were treated ± 1 mM metformin, then lysates were analyzed by immunoblot. **(E)** Ovx mice bearing orthotopic bilateral E2-driven HCC-1500 tumors (~400 mm^3) were treated with EW ± metformin (~5 mg/d) for 6 d. Tumors were harvested, FFPE, and sections were stained by IHC for P-ACC_{Ser79}. Proportions of positively-stained cells were measured in 3 microscopic fields (200x magnification) per tumor, and the mean value was used for each tumor (shown as one point in graph). Horizontal bars indicate mean ± SD. In (A/E), groups were compared by *t*-test. *$p \leq 0.05$. n.s.- not significant.

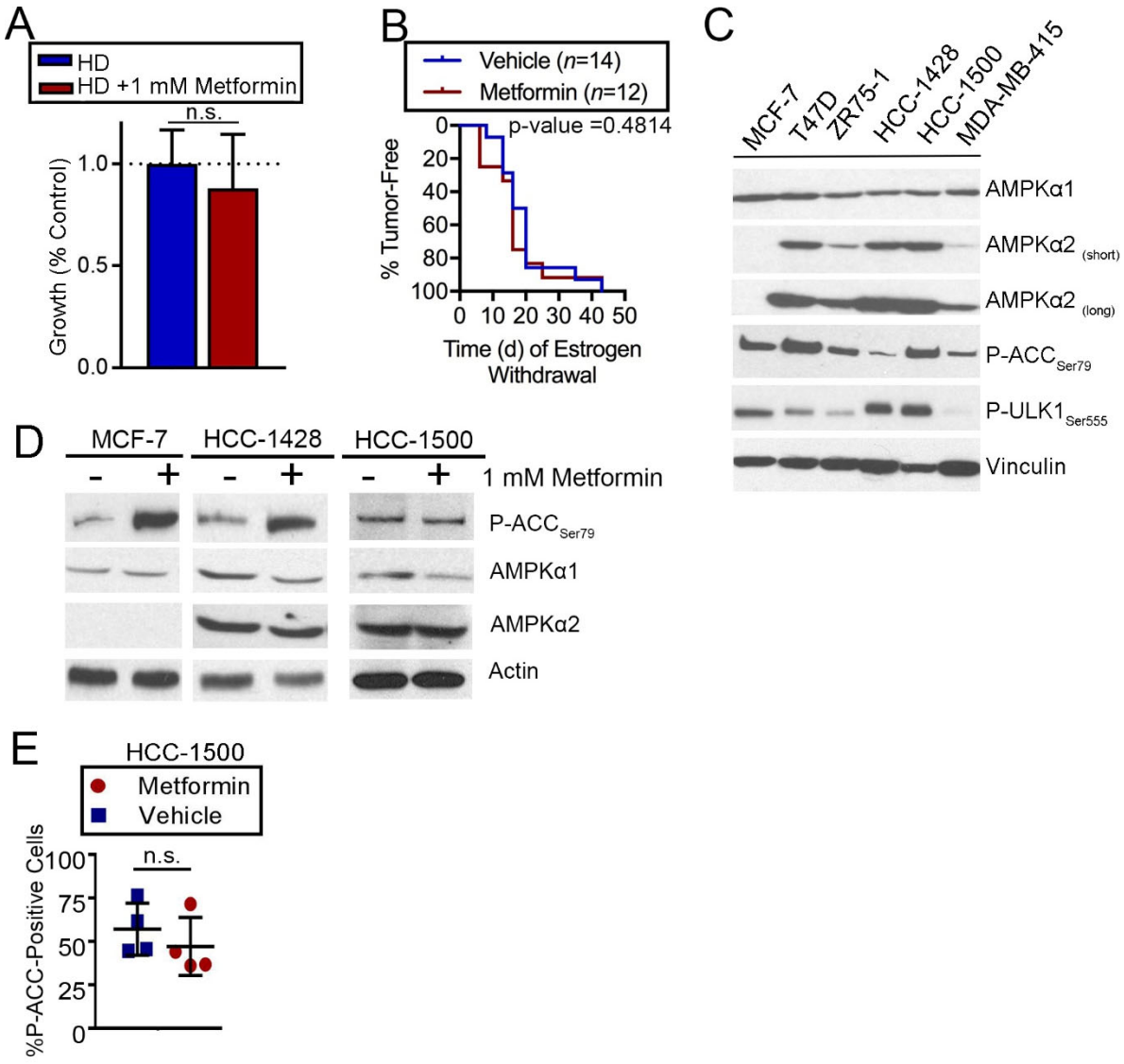

Figure S18. High-fat diet prevents estrogen withdrawal-induced regression of ER+ breast tumors. Ovx mice were conditioned to either a high-fat or low-fat diet for 2 wk, then injected orthotopically bilaterally with MCF-7 cells and implanted s.c. with an E2 pellet (with diet continuation). When tumors reached ~400 mm^3, mice were treated with EW (with diet continuation). Tumor volumes were serially measured, and groups were compared using non-linear effect modeling. $p\text{-value}_{RD}$ reflects differences between rates of tumor regression. Growth/regression curves of individual tumors are shown below.

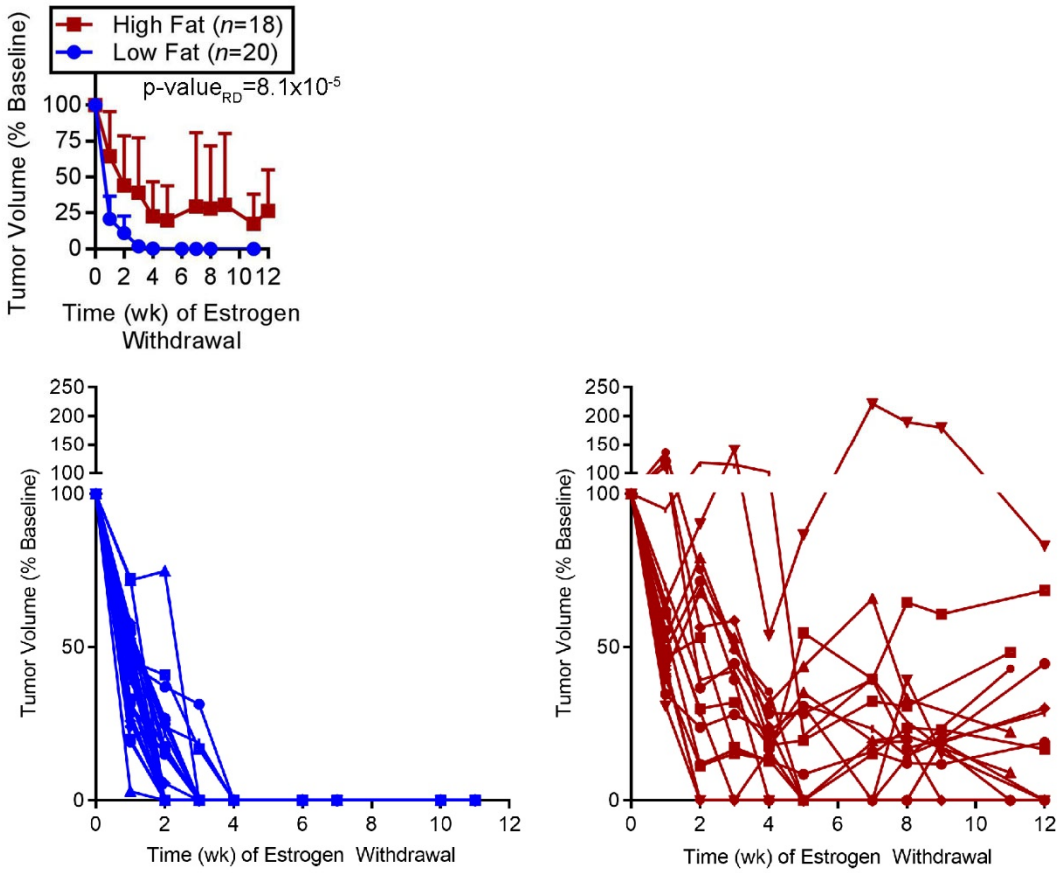

Figure S19. Immunohistochemical analysis of Ki67, CPT1α, and P-ACC in ER+ breast cancer xenografts treated with either high or low fat diets. Representative images for Ki67 **(A)**, CPT1α **(B)**, and P-ACC_{Ser79} **(C)** IHC staining of FFPE xenografts are shown. Tumor specimens were harvested from ovx mice on high-fat or low-fat diets following 0 or 90 d of estrogen withdrawal. Summarized data are shown in Fig. 7G-I.